



High precision tuning of RF cavity for 6 MeV SKKU X-band medical LINAC

Donghyup Ha¹ · SeungHyun Lee² · Mitra Ghergherehchi¹ · Sangbeen Lee² · Hyojeong Choi¹ · Ho Namgoong¹ · Jong-Seo Chai¹

Received: 24 February 2024 / Revised: 4 April 2024 / Accepted: 24 April 2024
© The Korean Physical Society 2024

Abstract

An X-band electron LINAC comprising 23 cells was fabricated and tuned for radiation therapy. The fabrication process used oxygen-free high-conductivity copper, which was divided into roughing and finishing stages to minimize machining errors. Resonance frequency measurements and tuning were performed for the half-cell, the unit cell with two half-cells combined, and all cells after assembly. Finally, the electric field inside the entire RF cavity was measured and tuned using a bead-pull test. The reason for the multi-step measurement and tuning was to minimize the number of tunings. Most of the tuning was done in the direction of increasing the frequency, and only a few were done in the direction of decreasing the frequency. All cells were tuned the same way. The finalized cavity had a resonance frequency of 9.306 GHz and a coupling coefficient of 1.277. Performance validation was performed through the percentage depth dose (PDD) test, confirming good agreement with the results for 6 MV X-rays.

Keywords Tuning · Radiation therapy · X-band · LINAC

1 Introduction

Radiation therapy is a well-known method for cancer treatment, and more than half of patients with cancer receive treatment through radiation therapy [1, 2]. Most radiation therapies are external beam radiation therapies, which use external radiation beams to target the patient's intended tissue or tumor site [3]. Radiation therapy includes proton and neutron therapies; however, X-rays are most widely used because of their accessibility and cost-effectiveness [4]. Electron linear accelerators are primarily used to generate X-rays [5].

Some commercial radiation therapy devices utilize linear accelerators operating in the C-band (4–8 GHz) or X-band

(8–12 GHz). However, most commercial radiation therapy devices that employ linear accelerators operate in the S-band (2–4 GHz). This is because they offer more alternatives for RF power and auxiliary components and exhibit a better tolerance for machining errors than higher frequency bands [6].

Since 2020, a dual-head gantry system for radiation therapy has been developed by Sungkyunkwan University. The dual-head gantry system is characterized using two X-ray sources. The two X-ray beams were designed to enhance the treatment efficiency [7]. This feature allows for reduced gantry movement time during treatment, flexible utilization of dosage, and the acquisition of various treatment angles. One X-ray source system incorporates various components, including RF power, cooling, vacuum, and shielding. The dimensions of the gantry were 2510 mm (width) × 2673 mm (height) × 1611 mm (depth), considering the building size. Inside the gantry, various systems such as the kV system, MV system, and positioning system are housed for precise treatment. Considering limited space, an X-band linear accelerator was used. The size of the RF system is determined based on the wavelength. Compared to the S-band, the X-band has a wavelength of approximately one-third, allowing for a more compact system configuration.

✉ Jong-Seo Chai
jschai@skku.edu

¹ Department of Electrical and Computer Engineering, Sungkyunkwan University, 2066, Seobu-ro, Jangan-gu, Suwon-Si, Republic of Korea

² Nuclear Physics Application Research Division, Korea Atomic Energy Research Institute, Daejeon, Republic of Korea

The reduction in the size of an X-band system implies an increase in manufacturing complexity. Typically, a machining error of 0.001 inch (2.54 μm) results in a frequency change of 1 MHz in the S-band range, whereas in the X-band, it leads to a frequency change of over 10 MHz [8]. This error is negligible in the case of the S-band. However, in the case of the X-band, an additional process for frequency tuning becomes essential.

This article outlines the construction and optimization procedures for an X-band linear accelerator (LINAC). The tuning process is systematically divided into four stages, each designed to minimize the overall number of adjustments. The three initial stages focused on fine-tuning the resonance frequency of the RF cavity, whereas the final stage involved a bead-pull test to enhance the uniformity of the electric field within the RF cavity. In this step, tuning was performed by comparing the internal field data acquired from the bead-pull test to the internal field data produced from the simulation. The performance of the X-band LINAC was validated using a percentage depth dose (PDD) test.

2 Specification of 6 MeV X-band LINAC

The electron linear accelerator was designed based on a magnetron (L-6170) with a power of 1.7 MW, and the X-band (9.3 GHz) was used for system compactness. The X-band LINAC was developed for radiation therapy to achieve an X-ray dose rate of over 800 cGy/min at a reference source-to-skin distance (SSD) of 85 cm using a beam energy of 6 MeV and a peak beam current of 70 mA.

The developed X-band LINAC consists of 23 cells, comprising 5 buncher cells and 18 accelerating cells. One of the accelerating cells is a coupler cell. In the cells, a beam hole with a diameter of 4 mm was designed to maximize the shunt impedance. Five buncher cells were designed to minimize the beam size while reaching 1 MeV to minimize the collisions between the beam and cells. A symmetrical structure with ports on both sides is used for the coupler cell. One port excites power, whereas the other functioned as a vacuum port. The symmetrical structure reduces field asymmetry, thus improving beam trajectory distortion [9, 10]. The accelerating cell consisted of 18 cells, which were designed to target a beam energy of 7 MeV to account for manufacturing errors. The overall structure of the X-band LINAC RF cavity is shown in Fig. 1.

3 Fabrication and calibration

3.1 Fabrication and tuning process

The sequence of activities for fabrication and optimization includes the following steps: fabrication of the RF cavity, measurement and tuning of half-cells, measurement and tuning of unit cells, measurement and tuning of full cells, bead-pull test and tuning, and RF characteristic measurement, as illustrated in Fig. 2.

The main considerations in the RF cavity fabrication process are the material to be used and the minimization of machining errors. The fabricated RF cavity cells were composed of side coupled cell (SC) and accelerating cell (AC). After the fabrication was completed, each half-cell

Fig. 1 Overall structure of X-band LINAC RF cavity

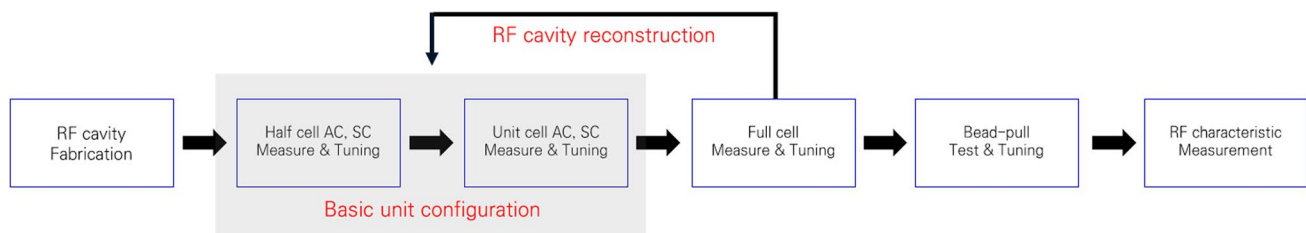
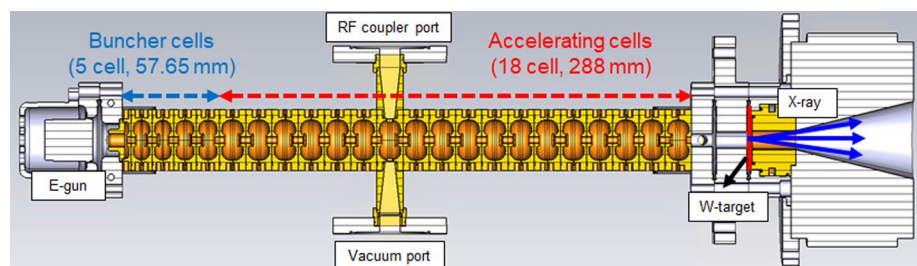


Fig. 2 Fabrication and tuning process

was measured and tuned. This step checks and tunes the difference between the frequencies of the designed and fabricated cells. After measuring and tuning the half-cell, it is measured and tuned again relative to the unit cell, which is a combination of two half-cells. There were three main reasons for this observation. When the LINAC was running, the default unit was the unit cell. Second, when a half-cell and a half-cell are combined, three resonance cavities are connected. These three resonance cavities could generate and verify the $\pi/2$ mode used by the developed RF cavity. The third reason is that the number of tunings can be reduced using the unit cell, compared to tuning each half-cell individually. The parameters vary when designing an X-band RF cavity, but some are designed with a 1 μm difference. Even if fabrication is completed using diamond tips, errors are inevitable. When measuring a half-cell, some will have a higher frequency than the designed frequency, and some will have a lower frequency. When these two half-cells are combined, an average value is obtained in the unit cell, thereby reducing the number of tunings. After the basic unit configuration through two iterations, the next step was to determine the assembly sequence of the entire cell by rearranging the order of the unit cells. The assembly sequence of a unit cell affects the number of cells required for tuning. The goal was to determine a combination that minimized the need for

tuning. Once the full-cell configuration is complete, repeat the measurement and tuning.

The brazing process proceeds after the full-cell process. After brazing, we used bead-pull measurements to measure and tune the field inside the RF cavity. When the bead-pull measurements and tuning were complete, the characteristics of the final RF cavity were measured.

3.2 Fabrication

Oxygen-free high-conductivity copper (OFHC) was used for production. OFHC have high electrical and thermal conductivities, and produce a relatively low number of secondary particles. Using a frequency of 9.3 GHz meant that ultralow errors were allowed in the fabrication. Various variables are used in the design of the X-band LINAC, and the minimum variation of variables is required to be 0.001 mm. This implies the machining error must be 0.001 mm or less for fabrication, as designed. The AC and SC half-cells were fabricated as one cell, as shown in Fig. 3a, b. The LINAC was produced using 23 unit cells, as shown in Fig. 3c. To minimize machining errors, the fabrication process was divided into two stages: roughing and finishing. Diamond tips were used for finishing to minimize machining errors. The fabrication process was carried out through the Variaxis

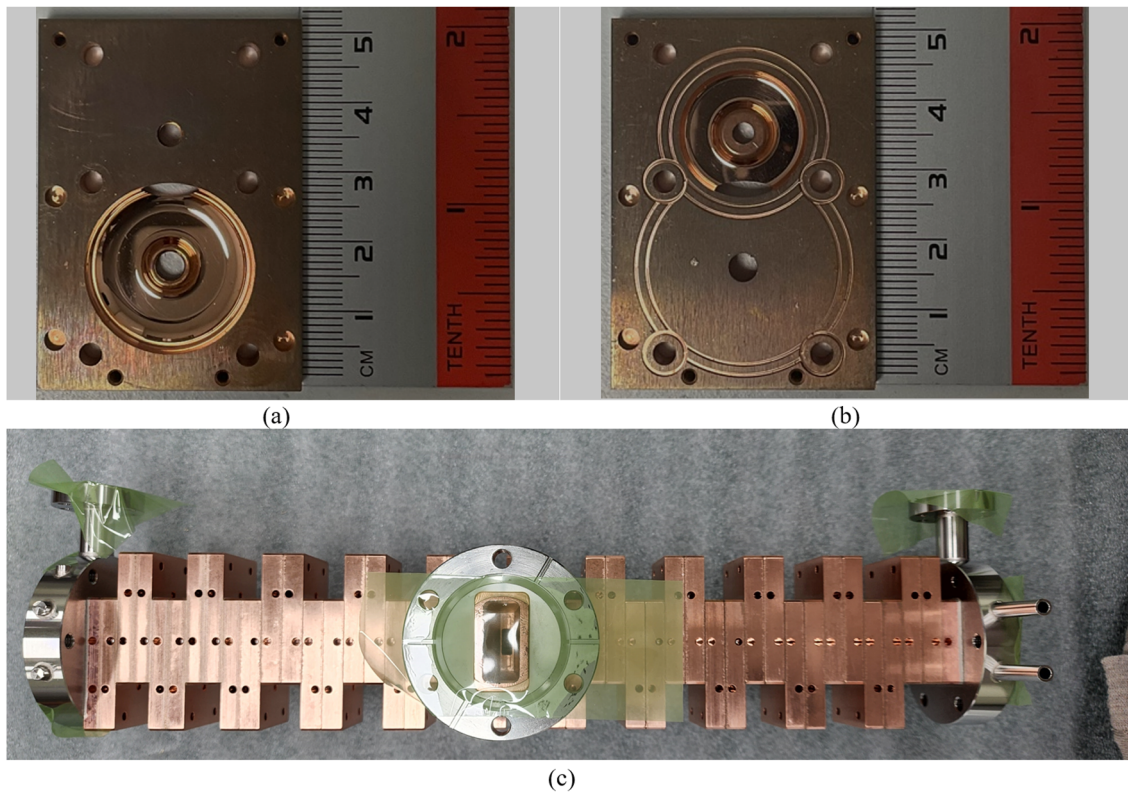


Fig. 3 Fabricated X-band LINAC: (a) AC half-cell, (b) SC half-cell, (c) complete X-band LINAC structure

i-600 from Mazak, a five-axis CNC machine. In the case of the buncher cell, it is difficult to solve the resonance frequency problem with a combination of half-cell and half-cell because the same cell is not repeated. However, in the case of the accelerating cell, it is often possible to solve the resonance frequency problem with a combination of half-cell and half-cell because the same cell is repeated. The fabrication was made with double the required cell in the case of the buncher cell, and the accelerating cell was made with 1.2 times (Table 1).

3.3 RF cavity measurement and tuning

In the Fig. 4a, the solid lines represent the tuning for a frequency increase, whereas the dashed lines represent the tuning for a frequency decrease. The tuning method was uniformly applied to all the cells. For frequency-increase tuning, an external force was applied inward to the RF cavity through a metal bead, causing it to deform. Figure 4b and c shows the tuning process for the frequency increase, inserting the metal bead into the hole shown in Fig. 4b and rotating the rod, as shown in Fig. 4c. The rod was threaded and exerted a downward force depending on the angle at which it was turned. Three tuning holes were created for

each half-cell, and each hole allowed a maximum frequency increase of up to 10 MHz per half-cell.

For frequency-decrease tuning, the flat region inside the cells was shaved off. This process involves mechanical machining and cannot be performed after assembly. Thus, it is the first step after identifying the required cells.

In the case of flat region tuning, because immediate frequency changes could not be observed during the tuning process, a trial was conducted using two cells to understand the trends before proceeding. On average, a change of 10 μm resulted in a frequency shift of approximately 0.9 MHz, as shown in Fig. 5.

Figure 6 shows the method for measuring the resonance frequency of a half-cell using a vector network analyzer. The measured data were compared with the design values. It exhibits different values up to 20 MHz, as shown in Fig. 7a.

The unit cell consists of the largest value in the positive direction and the largest value in the negative direction based on the half-cell measurement result. For example, there are four cells and each of the four cells has resonance frequencies of -10 MHz, -7 MHz, $+9$ MHz, and $+6$ MHz relative to the reference frequency. Positive

Table 1 Specification of the designed X-band LINAC

	Parameter
Unloaded Q factor(Q_0)	7886
Coupling beta (β)	1.328
Operating frequency	9.3 GHz
Dose rate (@ SSD=85 cm)	800 cGy/min
Beam size (full width at half maximum)	0.45/0.45 mm
Output beam energy	> 6 MeV
Beam current (peak)	70 mA
Input RF power	1.7 MW
Operating mode	Standing wave, $\pi/2$ mode
Structure type	Side-coupled type
E-gun voltage	12.5 kV
Length of LINAC structure	345.65 mm

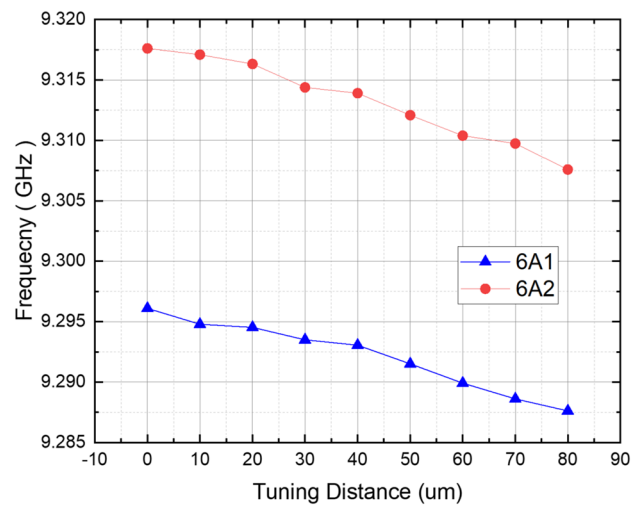
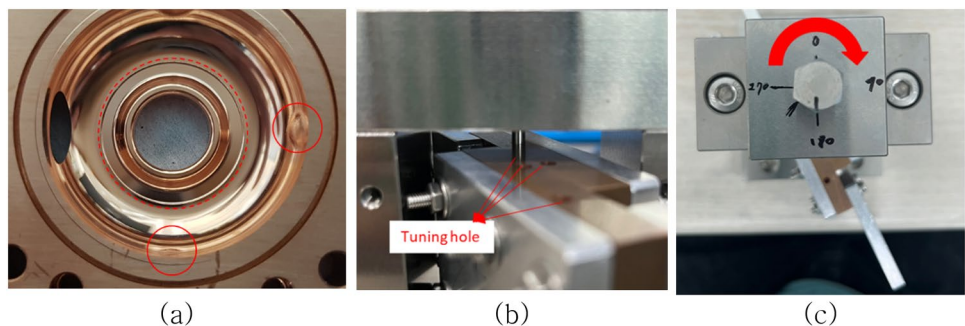


Fig. 5 Tendency to frequency down

Fig. 4 Tuning method and position: (a) tuning position, (b) tuning method with side view, (c) tuning method with upper view



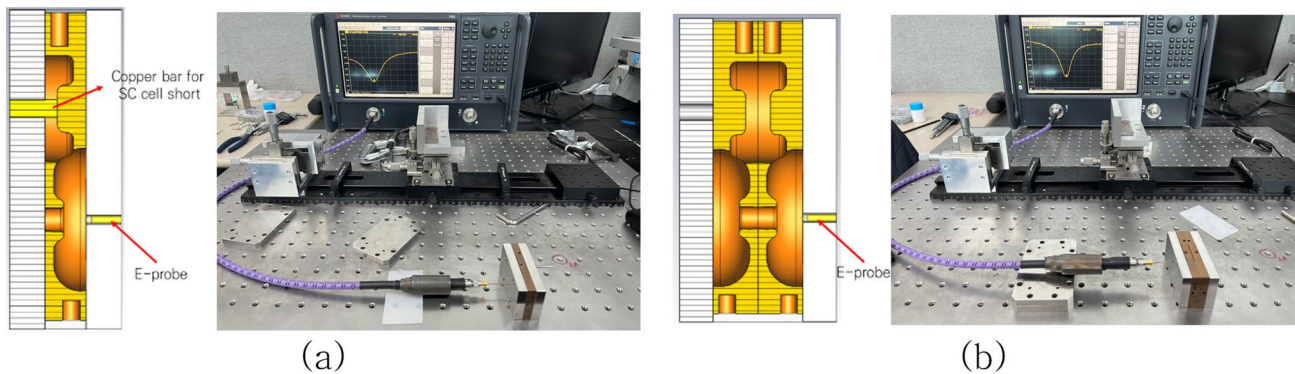


Fig. 6 Frequency measurement set up: (a) half-cell, (b) unit cell

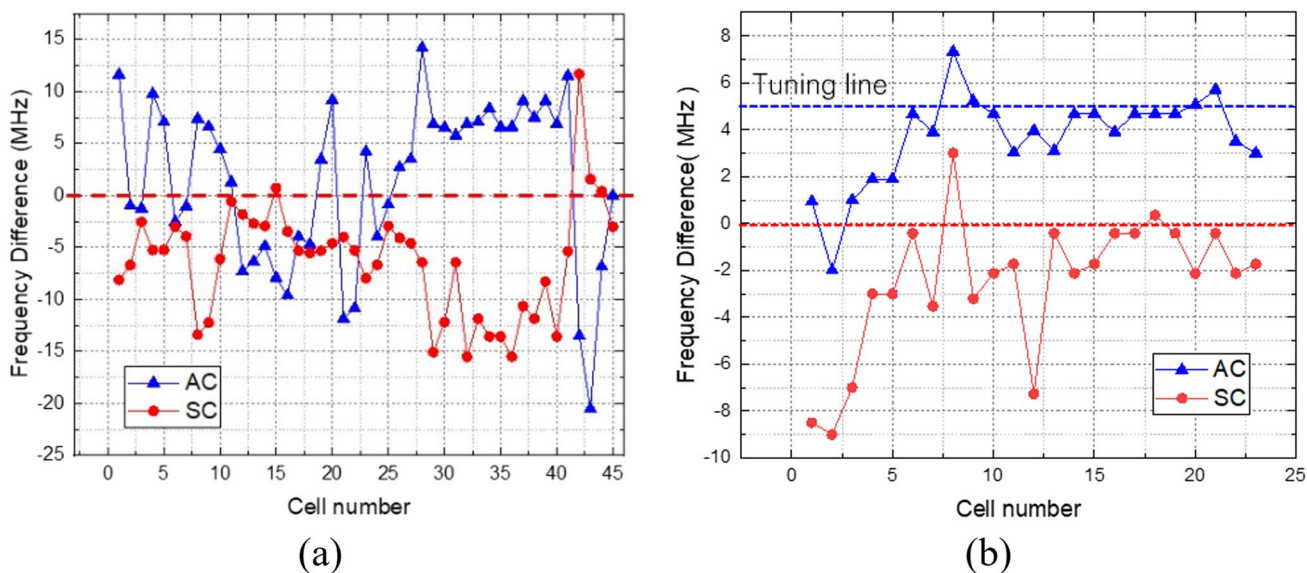


Fig. 7 RF cavity measurement results: (a) half-cell, (b) unit cell

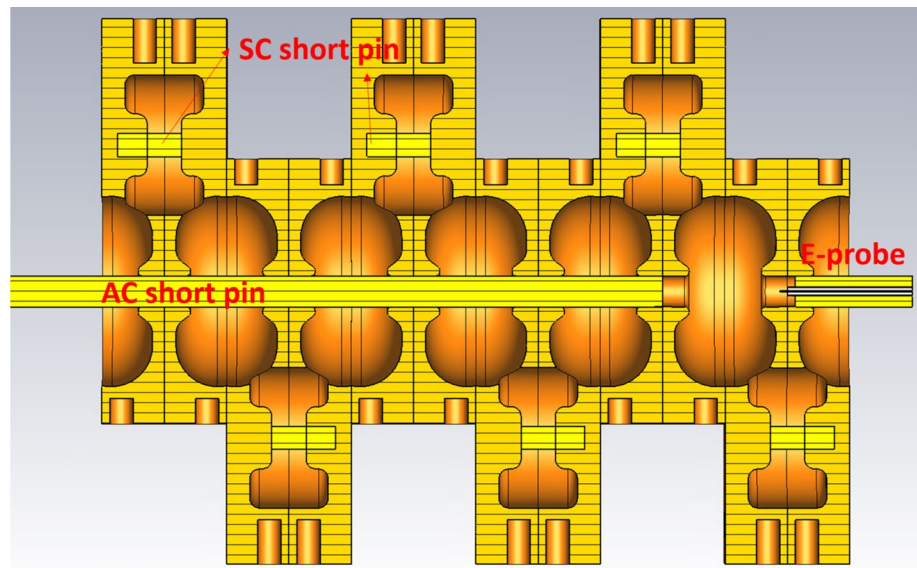
direction means + direction, and negative direction means - direction. Based on the four cells, - 10 MHz and +9 MHz, - 7 MHz and +6 MHz combine to form two unit cells. This process was applied to the entire set of cells, resulting in the graph depicted in Fig. 7b. Figure 7 shows that (b) has a reduced deviation compared to (a). Based on the accelerating cell, the tuning frequency was chosen to be 9.305 GHz, which is 5 MHz above the reference frequency. Tuning was performed using the method in Fig. 4. The entire cell was assembled, measured, and tuned as a final check before brazing. Figure 8 shows the AC measurement method used when the full cell was assembled. For the SC measurement, the SC frequency was measured at the SC short-pin position after shortening the AC. Using this method, we measured all the cells and verified that the values measured and tuned in the unit-cell step were correct. Figure 3 shows that each cell has four pinholes to guide the alignment during assembly.

Although there are pins for alignment, this method was used for the final confirmation because the RF cavity is fixed after brazing, and modifying it later is difficult. After the unit-cell measurement and tuning were completed, the frequency and coupling beta values of the coupler cell were measured, and values of 9.305 GHz and 1.2 were obtained, respectively.

3.4 Bead-pull test and tuning

The brazing process was completed after tuning, as shown in Fig. 3c. After brazing, the field distribution inside the RF cavity was measured using a bead-pull method based on the Slater perturbation theorem [11]. The bead used was a metallic sphere with a diameter of 1.55 mm, and a polyester series with a diameter of 0.55 mm was used for the string. The tuning was performed by comparing the measured

Fig. 8 AC measurement method at a full cell



and designed field distributions. The final state is shown in Fig. 9.

The frequency was adjusted through the previous three stages, but a difference between the initial state and the simulation data was found. This is because the frequency compounds the field magnitude inside the RF cavity, the degree to which the AC and SC cells are coupled, the electric field, the magnetic field, and the bead size. [12, 13] In addition, distortion can occur due to the expansion and contraction of cells during brazing. It is recommended to change the size of the AC and SC coupling slots for field-flatness tuning; however, after brazing, the location of the coupling slots is not visible outside, and the location is deep inside, making direct tuning difficult. Therefore, the field magnitude was adjusted using additional frequency tuning.

The entire electric field distribution was tuned to achieve a field flatness of less than 5%. When comparing the initially measured field distribution with the simulated field

distribution, the most significant difference was observed between the first and last cells, as shown in Fig. 9b. The first cell exhibits a difference of 15% in the simulations. Excluding these two cells, the remaining cells did not show significant deviations from the simulation results. The tuning was focused on the first and last cells, which differs by 4.8% from the simulation. The final state of field distribution is shown in Fig. 9c.

4 Experimental result of RF cavity

After completing the tuning process, including the bead-pull test, the X-band RF cavity characteristics were measured using a network analyzer. The value of S11 was measured at -18.34 dB at 9.306 GHz, and the coupling state was measured in an over-coupled state with an SWR (standing wave ratio) of 1.277 as shown in Fig. 10.

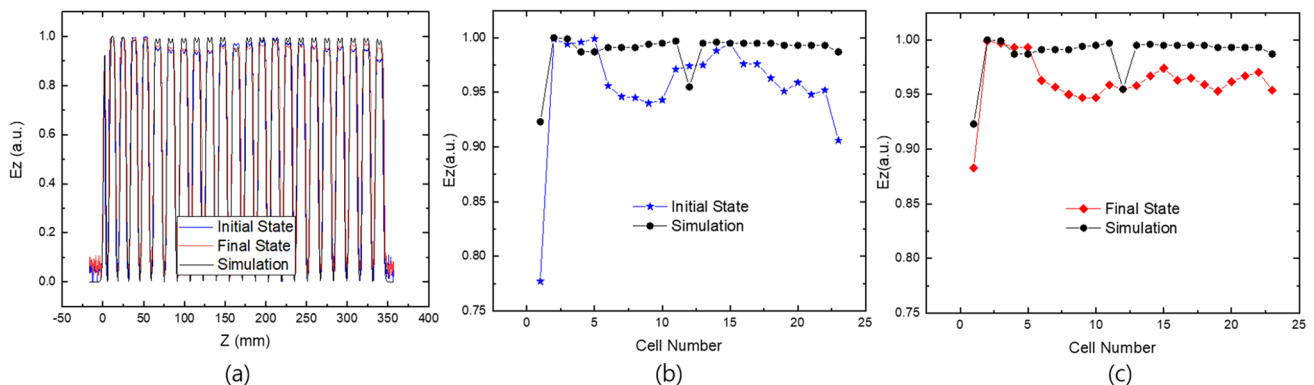


Fig. 9 Electric field distribution in the X-band LINAC. (a) On-axis E-field distribution, (b) initial state with the simulation, (c) final state with the simulation



Fig. 10 Measurement of X-band LINAC characteristics with network analyzer: (a) S11, (b) SWR

A test bench was set up to match the actual operating conditions, as shown in Fig. 11a. The electron beam is generated from a 12.5 kV DC electron gun and enters the X-band RF cavity, which consists of 23 cells. Among these, the 12th cell is a coupler cell, housing two ports. The first port is the power coupler port, where power is fed and connected to a magnetron through a WR 112 waveguide. The other port is a vacuum port connected to a turbomolecular and a rotary pump. An ion pump was installed to maintain a vacuum state of pressure less than 10^{-8} torr. The cooling system is constructed using deionized water to

maintain a system temperature of 28 °C. The beam entering the X-band RF cavity was accelerated to more than 6 MeV, collided with the tungsten target, and was converted into bremsstrahlung X-rays.

The PDD curve for radiation therapy is crucial for treatment planning. This information is vital for determining the appropriate treatment depth and dosage for effective delivery to the target area while safeguarding healthy tissues and organs. The PDD curve was measured using a solid water phantom at an SSD of 100 cm. The doses at

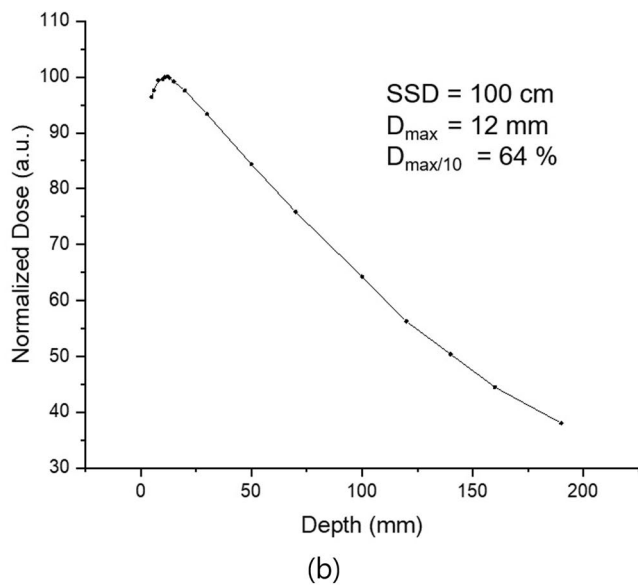
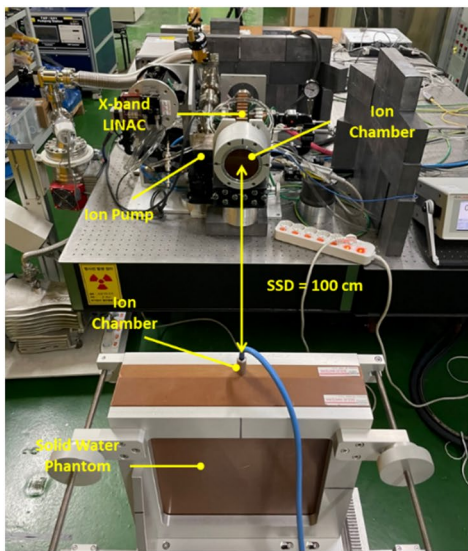


Fig. 11 PDD test: (a) PDD experiment test bench, (b) PDD result

Table 2 Final results of X-band LINAC between the designed and fabricated value

	Designed	Fabricated
Unloaded Q factor (Q_0)	7886	7046
Coupling beta (β)	1.328	1.277
Operating frequency	9.3 GHz	9.306 GHz
Dose rate(@source-to-object distance = 850 mm)	800 cGy/min	890 cGy/min
Output beam energy	> 6 MeV	> 6 MeV
Input RF power	1.7 MW	1.5 MW
Operating mode	Standing wave, $\pi/2$ mode	
Structure type	Side-coupled type	
E-gun voltage	12.5 kV	
Length of LINAC structure	345.65 mm	

each point were measured using an ion chamber, and the results are shown in Fig. 11b.

The PDD test was performed with a magnetron power of 1.5 MW and a 2 mm thick copper plate installed after the target. When the PDD test was performed according to the design specifications, that is, a magnetron power of 1.7 MW and no copper plate, the electrons continued to penetrate the target, and a PDD curve was not formed.

The depth of the PDD test was measured from 5 to 190 mm. The maximum dose rate was observed at a depth of 12 mm. At a depth of 100 mm, it reached 64% of the maximum value. Typically, for a 6 MV medical linear accelerator, the maximum dose rate occurs at a depth of 13–15 mm [14]. This data confirmed that the generated beam was near 6 MV energy. With a magnetron power of 1.7 MW and considering the additional 2 mm thickness of the metal plate, it can be inferred that the developed accelerator can produce X-rays exceeding 6 MV. However, experiments need to further confirm this after optimizing the tungsten target thickness.

The ion chamber recorded a measured dose rate of 6.47 Gy/min at an SSD of 100 cm. When adjusted to an SSD of 85 cm, this value increased to 8.9 Gy/min, satisfying the targeted dose rate. As summarized in the Table 2, the manufacturing and experimental processes validated the strong alignment between the designed and fabricated values.

5 Conclusion

This study describes the fabrication, tuning, and validation of an X-band linear accelerator operating at a frequency of 9.3 GHz as an X-ray source for radiation therapy. Following fabrication, there was an approximately 10 MHz discrepancy from the reference frequency. Various measurements were conducted to minimize the number of tuning iterations, including half-, unit-, and full-cell measurements. After

completing these steps, the electric field generated within the RF cavity was verified by bead-pull tests. A comparison between the measured and simulated electric fields guided additional tuning. Upon final tuning, the field flatness was within 5%. After completing all the tuning processes, the RF cavity frequency characteristic was 9.306 GHz. This discrepancy from the original RF cavity measurement was 1 MHz higher in the reference value setting, and additional tuning during the bead-pull process contributed to the frequency increase. Subsequently, the suitability of the developed X-band RF cavity as a medical accelerator was verified using PDD measurements. The PDD results confirmed that the developed X-band LINAC generates 6 MV X-ray. The developed RF cavity was optimized using a tungsten target and experimental conditions. Subsequently, it was integrated into a gantry and subjected to quality assurance procedures in a real treatment environment.

Acknowledgements This work was supported by a grant from the Korea Medical Device Development Fund, funded by the Korean government (Ministry of Science and ICT) (Project Number: 1711135001, KMDF_PR_20200901_0042).

Declarations

Conflict of interest The authors declare the following financial interests/personal relationships which may be considered as potential competing interests: Jong-Seo Chai reports financial support was provided by Sungkyunkwan University College of Information and Communication Engineering.

References

1. M.B. Barton, S. Jacob, J. Shafiq, K. Wong, S.R. Thompson, T.P. Hanna, G.P. Delaney, Estimating the demand for radiotherapy from the evidence: a review of changes from 2003 to 2012. *Radiother. Oncol.* **112**(1), 140–144 (2014)
2. R. Atun, D.A. Jaffray, M.B. Barton, F. Bray, M. Baumann, B. Vikram, M. Gospodarowicz, Expanding global access to radiotherapy. *Lancet Oncol.* **16**(10), 1153–1186 (2015)
3. P. Hoskin, *External beam therapy* (Oxford University Press, Oxford, 2019)
4. M. Goitein, M.J.C.O. Jermann, The relative costs of proton and X-ray radiation therapy. *Clin. Oncol.* **15**(1), S37–S50 (2003)
5. A. Wambersie, R.A. Gahbauer, Medical applications of electron linear accelerators (1996)
6. Y.S. Lee, S. Kim, G.J. Kim, J.H. Lee, I.S. Kim, J.I. Kim, Y.N. Kang, Medical X-band linear accelerator for high-precision radiotherapy. *Med. Phys.* **48**(9), 5327–5342 (2021)
7. S.H. Lee, S.W. Shin, J. Lee, H.S. Kim, B.N. Lee, B.C. Lee, J.S. Chai, X-band Linac for a 6 MeV dual-head radiation therapy gantry. *Nucl. Instrum. Methods Phys. Res. Sect A Accel. Spectrom. Detect. Assoc. Equip.* **852**, 40–45 (2017)
8. A. Chao, W. Chou, Reviews of accelerator science and technology, vol. 2 (2009)
9. R. Eichhorn, C. Egerer, J. Robbins, V. Veshcherevich, Design of a symmetric coupler for superconducting elliptical cavities. *IOP Conf. Ser. Mater. Sci. Eng.* **101**(1), 012099 (2015)

10. M.D. Forno, P. Craievich, G. Penco, R. Vescovo, Theoretical and experimental analysis of a linear accelerator endowed with single feed coupler with movable short-circuit. *Rev. Sci. Instrum.* **84**(11) (2013)
11. L.C. Maier Jr., J.C. Slater, Field strength measurements in resonant cavities. *J. Appl. Phys.* **23**(1), 68–77 (1952)
12. S. Som, S. Seth, A. Mandal, S. Ghosh, Bead-pull measurement using phase-shift technique in multi-cell elliptical cavity. *Proc. IPAC* **280**(282), 2011 (2011)
13. B. Zhou, P. Zhang, W. Li, H. Zhang, L. Zhang, S. An, Optimization and measurement for an electron side-coupled linac with longitudinally off-axis coupling cavities. *Nucl. Instrum. Methods Phys. Res. Sect A Accel. Spectrom. Detect. Assoc. Equip.* **987**, 164842 (2021)
14. S.V. Kutsaev, R. Agustsson, A. Arodzero, R. Berry, A. Bezh-anov, S. Boucher, K. Woods, Compact X-band electron linac for radiotherapy and security applications. *Radiat. Phys. Chem.* **185**, 109494 (2021)

Publisher's Note Springer Nature remains neutral with regard to jurisdictional claims in published maps and institutional affiliations.

Springer Nature or its licensor (e.g. a society or other partner) holds exclusive rights to this article under a publishing agreement with the author(s) or other rightsholder(s); author self-archiving of the accepted manuscript version of this article is solely governed by the terms of such publishing agreement and applicable law.